Egyptian Journal of Chemistry

http://ejchem.journals.ekb.eg/

Evaluation of the Upper Cretaceous Black Shales: A Case Study from Islam and Hamrawin Phosphate Mines, Qussier Area, Southern Eastern Desert, Egypt

Esmat A. Abou El-Anwar[a,*]

[a] *Geological Sciences Department, National Research Centre, Dokki, Giza, Egypt*

Abstract

The Campanian-Maastrichtian parent rock of Islam and Hamrawin Mines shale from Qussier was studied from mineralogical and geochemical compositions to deduce its origin, deposition environments, tectonic setting, as well as the economic evolution. XRD patterns indicated that the study black shales are consisted of two phases, clay and non clay minerals. The Duwi Formation implies highly textural maturity. The black shales for Duwi Formation were formed under anoxic shallow marine conditions. The chemical parameters indicated that the study area was deposited under high salinity, warm and humid climate conditions. The high Fe_2O_3 content, some traces and REEs; Zr, Ba, Nb, Sr, Ce, Th, Y, Hf, and La concentrations as well as ICV and CIW pointed to input of recycling components derived from old sedimentary basins in a comparatively stable tectonic setting. The geochemical data, CIA, CIW and PIA values are revealed that the Duwi Formation black shales are subjected to the intensive chemical weathering either for the original basis or through transportation before deposition. The studied samples are plot in active continental margin of provenance. Black shales of Islam mines are represent the highest average of ΣREEs, ΣLREEs and ΣHREEs (233.75, 125.67 and 41.72ppm; respectively), with respect to the other neighboring mines. Consequently, the ΣREEs are increased to the direction of south Qussier. The chemical composition of black shales for the Duwi Formation had diversity sources for redox-sensitive traces and REEs in the Qussier area. Black shales of Islam and Hamrawin Mines can be classified as high-quality sources for extraction oil and gas.

*Keywords:*Duwi Formation, Qussier, Black Shales, Anoxic, REEs

1. Introduction

The traces REEs are applied to explain sedimentary environment, process and structural setting of depositional basins. REEs are also used as important tools in delineating the geochemical environment during the formation of authigenic and diagenetic minerals [1,2,3]. Rare earth elements (REE) are known to be more resistant to fractionation by weathering and metamorphism than any other trace element [4]. Black shales, with a wide global distribution, were mainly deposited in relatively deep, anoxic basins [5]; where sediment accumulated most of the times very slowly. Black shales are often enriched not only in OM (organic matter) but also in trace elements like Co, Cr, Cu, Mo, Ni, V, Mn and Zn. These elements usually show positive correlation with OM and/or sulphides. Because of high organic carbon and sulphide contents, black shales are subject to alteration when exposed, and mining in shales throughout the world has accelerated the weathering of these sedimentary rocks. The weathering can disperse the toxica metals hosted in the shales; and thus, some metals can be lost from shales and others are enriched.

The black shales from Duwi Formation (Campanian-Early Maastrichtian) in the region of Qussier-Safaga in Easten Desert, Egypt attracted the attention of previous authors to evaluate it as well as their economic impact as a basis rock and raw material [6,7,8,9,10,11,12,13,14,15,16].

As far as the author is aware, the published data on the geochemistry of the Islam and Hamrawin Mines black shales are definitely insufficient. However, the

*Corresponding author e-mail: abouelanwar2004@yahoo.com.; (Esmat A. Abou El Anwar).
Receive Date: 23 February 2022, Revise Date: 17 April 2022, Accept Date: 24 April 2022.

DOI: 10.21608/EJCHEM.2022.123645.5523

©2019 National Information and Documentation Center (NIDOC).

geochemistry work was studied the Qusseir region as a general [17, 18, 16, 14].

Thus, the chief aim of the present article is to give detailed geochemical explanation on the black shales of Islam and Hamrawin Mines, Duwi Formation at Qusseir area, in an attempt to recognize its depositional environment and the economic evolution. Also, try to discuss some aspects concerning the depositional environments during the precipitation of the Duwi Formation.

1.1.Geology of the area

Black shales occur in Egypt in numerous localities and at dissimilar geologic ages. The Carbonaceous shales have a broad distribution on the Egyptian surface and subsurface. They were extant in age from Carboniferous to Eocene. The phosphorites are intercalated with and capped by black shales. They have significant amounts of organic matter and are enriched in the trace elements; thus could be of economic potential. The Upper Cretaceous sediments in southern Egypt consists of variegated shales which, upon a thick sedimentary succession follow. These sediments are of shallow origin with some vertical and lateral lithological changes, in which the phosphate deposits are, intercalated [19]. The compositions of shales could provide information on the tectonic setting, provenance, weather conditions, pollution and sediment recycling.

In Egypt, shales occur in an east-west trending belt extending from the Quseir-Safaga district along the Red Sea to the Kharga-Dakhla land-stretch passing through the Nile Valley. The black shales are hosted mainly in the Campanian to Maastrichtian Duwi and Dakhla formations. Duwi Formation, a part of this sequence, is composed of interbedded shales, reefal-limestone, marls, as well as phosphatic bands. The Duwi Formation is conformably overlain by the Qusseir variegated shales and underlain by the Dakhla shales in the Qusseir-Safaga area [20].

Generally, shale is an expression used to point to several mudrock having fissility. The characteristic tint of shale is graduated from grey to black. Black shales have > 1 % organic matter, thus the color revealed a reducing environment. Thus, drab color can be interpreted to maceral (organic matter) occurrence of >1 [8]. The chosen area is represented by Islam and Hamrawin Mines (Fig. 1). They occur at the Upper Member of Duwi Formation (Fig. 2) in Qusseir-Safaga locality (Baioumy and Tada, 2005) [20].

2. Materials and Methods

Geological field trips were done for study the geologic setting and collecting some representative rock samples of the black shale from Islam and Hamrawin Mines. Twenty distinctive samples were collected. Ten samples collected from each mine. The mineralogical components were investigated by the X-Ray Diffraction (XRD) technique for two samples at the Egyptian Mineral Resources Authority (Dokki,

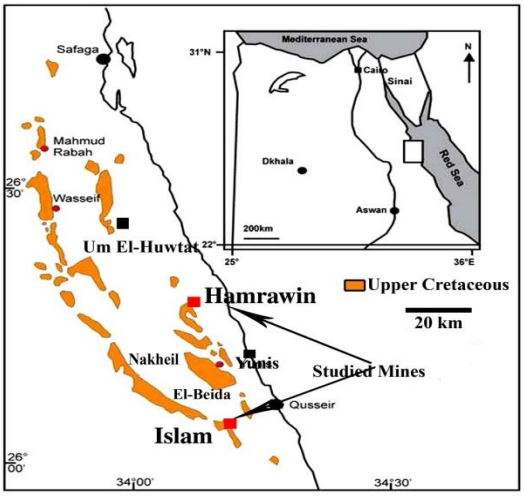

Fig. 1: Location map of Hamrawin and Islam Mines

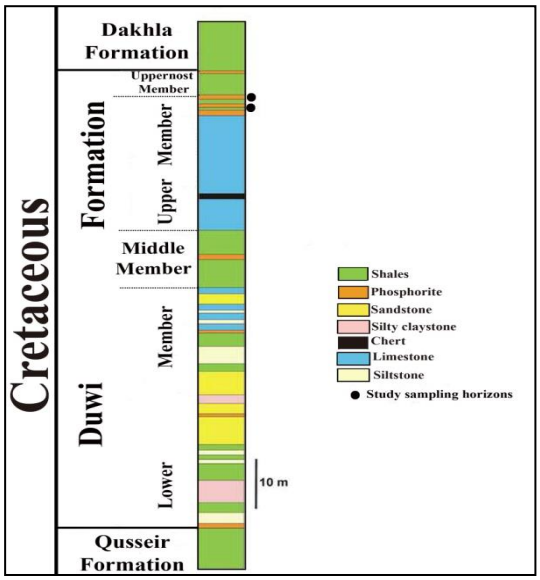

Fig. 2: Lithostratigraphic section of Duwi Formation in the Red Sea Region (modified after [20]).

Egypt) using a PAN analytical X-Ray Diffraction equipment model X'Pert PRO with Secondary Monochromator, Cu-radiation (λ=1.542Å) at 45 K.V., 35 M.A. and scanning speed 0.02o/sec. were used. The diffraction charts and relative intensities are obtained and compared with ICDD files. In addition, SEM-EDX analysis were also carried out for two samples to study the morphology and the size of the synthesized samples were characterized via SEM coupled with energy-dispersive spectroscopy EDX, (SEM Model Quanta FEG 250) are carried out in the National Research Center laboratories. Twelve represented samples were chosen for the geochemical components were delineated by X-Ray Fluorescence (XRF) technique to determine the chemical composition by using Axios Sequential WD_XRF Spectrometer, Analytical 2005 in the National Research Center laboratories, with reference to the ASTM E 1621 standard guide for elemental analysis by wavelength dispersive X-ray fluorescence spectrometer and ASTM D 7348 standard test methods for loss on ignition (LOI) of solid combustion.

3. Results and Discussion

3.1. Mineralogy

The mineralogy of the studied samples, from the Islam and Hamrawin Mines black shales are presented in Fig. 3. XRD results indicated the prevailing clay minerals from the two mines were comprised of montmorillonite and kaolinite. Kaolinite is traditionally formed in tropical to subtropical humid climatic environments [21]. Non-clay minerals of the study black shales were consisted mostly of quartz, gypsum, pyrite and calcite.

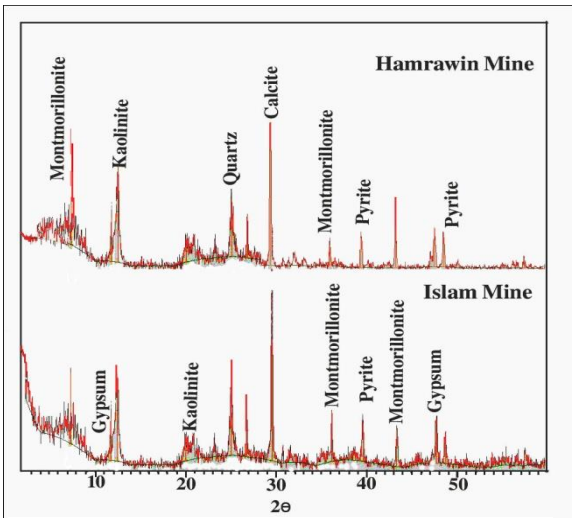

Fig. 3: X-ray diffractograms for the sample Nos. (4) and (9) of Hamrawin and Islam mines; respectively.

SEM results of the studied samples confirmed the dominance of montmorillonite, (Figs. 4a and b), which conformed to XRD analyses. The montmorillonite and Kaolinite presents as detrital and authigenic origin (Fig. 4a). The great quantity of montmorillonite pointed to deposition beneath a marine condition, and in warm/humid climate [22, 23]. Also, Figure (4a) shows and halite crystals and quartz grains. Pyrites occurs as framboidals (6 µm), are pseudomorphosed and are occurred authigenically, which conformed to XRD analyses (Fig. 4b). The spherical shape of pyrite crystals is indicating shallow marine reducing environment through the deposition [10, 24].

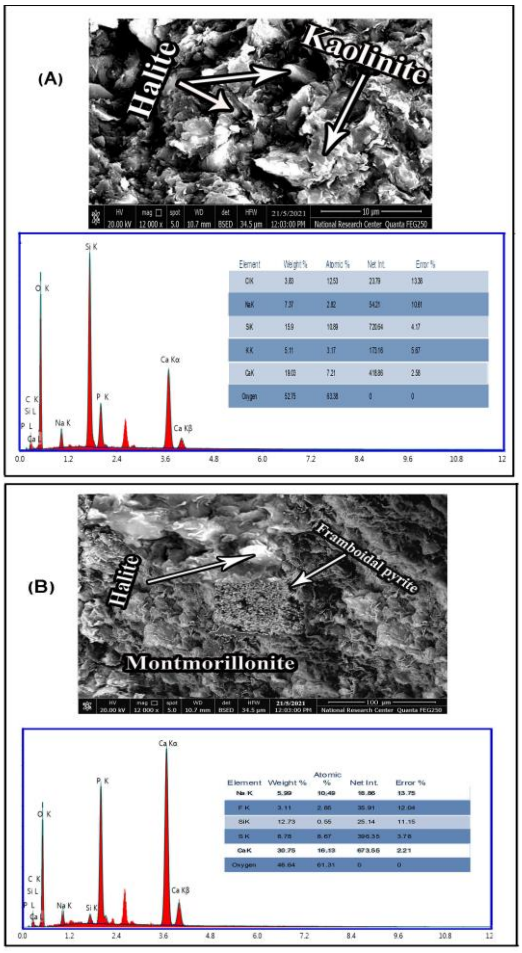

Fig. 4: A): BSE image and EDX analysis data showing a dominance of the montmorillonite and Kaolinite occur as detrital origin as well as quartz grains and halite crystals in the matrix (Sample No. 5). B) BSE image and EDX analysis data showing a

framboidals pyrite and quartz grains scattered in the montmorillonite matrix, Ca (30. 75%), S (8.78%), Si (12.73%), Fe (3.11%) and Na (4.2%), (Sample No. 11).

3.2. Geochemistry

The major, traces and REEs chemical compositions within the Islam and Hamrawin mines, in addition to their ratios, are quoted in Table 1. The spider diagram of these elements is shown in Table 2.

Islam samples are enrichment content in SiO_2, Al_2O_3, MgO and Fe_2O_3 than those of the Hamrawin samples. In the other hand, Hamrawin samples are greatly concentrated in CaO, P_2O_5 and SO_3. The loss of ignition values was recorded averaged (25.06%) for the entire area.

The percentages of heavy metals; V, Mo, Zn, Cr, Pb, Zr, Cd, Sr, As, Se, and rare earths; Y, Sm and U in the studied area are elevated than those of Upper Continental Crust (UCC) and for the Post Archaean Australian Shale (PAAS) [25, 26], Fig. 5. The percentages of Mn, Ba, Pb, Co, Rb, Hf, Nd, and the REEs; Sc, Ce, La, Nb and Th were lower than those of (UCC) and/or (PAAS) for the study area (Fig. 5).

3.2.1. Major elements

SiO_2, Al_2O_3, MgO and Fe_2O_3 (average 26.45, 15.90, 5.52 and 4.77%; respectively) are more enrichment for the studied Hamrawin samples compared to those of the Islam samples (18.67, 9.0, 1.9 and 2.70%; respectively) (Table 1). The Islam samples are more enhanced in CaO, P_2O_5 and SO_3 (average 28.90, 5.87, 1.90 and 3.67%; respectively), (Table 1). The studied shale in two mines of the study area are comparatively depleted in NaO_2, K_2O and TiO_2 (average 0.35, 0.9 and 0.27%; respectively), Table 1.

The high loss of ignition (average 22.1 and 28.03% for Islam and Hamrawin mines; respectively) and average 25.06% for the study area indicated to the present of great quantity of OM. During chemical weathering the microbes within black shales could be affected of the organic matter [27]. OM varies from 16.54 to 19.52 % and averaging 18.02 %.

Strong positive relation (r=0.96, Table 2) between SiO_2 and Al_2O_3 indicated that the majority Al_2O_3 is here as clay minerals, which conformed by XRD, occurring as well as detrital grains, which conformed to SEM results. Strong positive correlation (r=0.79) between Al_2O_3 and NaO_2 indicated predominant montmorillonite, which is most possibly as Na-montmorillonite, which conformed by XRD. The low average K_2O/ Al_2O_3 (0.07) is revealed that occurrence of kaolinite mineral in the studied samples which conformably by XRD. Also, there is no relation between Al_2O_3 and K_2O indicated absence of illite minerals which conformably with XRD, where it is not detected with XRD. Also, strong positive correlation (r=0.94) between CaO and SO_3 indicated that occurrence of gypsum which conformably with XRD and agrees with [28, 29, 30, 16, 31, 13]. Moderate positive relation (r=0.30) between NaO_2 and Cl pointed out to the presence of halite the studied black shales which conformably with SEM examination.

Average value 3.73% for Fe_2O_3 was quoted in the study samples. This percentage possibly will be resulted from hydrothermal leaching or additions of Fe, conformed by reduced fluids [32, 26, 14]. The strong positive correlation (r = 0.94) between OM and SO3 content indicates that the organic sulfur prevails along with pyrite [33, 16].

3.2.2. Traces and Rare Earths (REEs)

The most abundant trace element in the study black shale samples is V, average 1099.1 ppm, and high positive correlated with OM (r= 0.97). The elevated percentage of V may be the product of oxidation as well as weathering of organic matter [34, 35]. Zn considered the second mainly rich trace element in the studied samples (average 1095 ppm). The higher content of Zn, and the strong positive correlation incorporated with apatite and organic matter (Table 2). In the other side, REEs recorded low percentages <100 ppm, which ranging from averages (1.04ppm) Hf to (32.12ppm) of Ce for the black shales of the study area (Table 1 and Fig. 5).

Black shales in the Islam mines are highly enriched in traces {(Zr = 478.33, Pb =9.47) and (Ba=80.5 ppm)} as well as rare earths (Y= 32.5, Hf = 1.24, As = 11.62, Rb = 34.5, Ce = 46.5, La= 38, Sc = 9.22, Ga = 20, Sm = 10.55, Nb = 8.96 and Th = 8.93 ppm) compared to those of the Hamrawin mines (Table 1 and Fig. 5).

Table 1: The chemical composition of major oxides (%), traces and REEs (ppm), essential ratios CIA, CIW and ICV of studied black shales samples in Hamrawin and Islam mines

	Hamrawin Mine							Islam Mine						
S. No.	**1**	**2**	**3**	**4**	**5**	**6**	**Average**	**7**	**8**	**9**	**10**	**11**	**12**	Average
SiO_2	25.10	26.80	25.50	25.90	26.10	29.30	26.45	19.10	17.50	18.90	18.50	19.90	18.10	18.67
Al_2O_3	15.10	16.80	15.60	15.90	16.20	15.80	15.90	8.40	8.10	8.80	9.10	9.70	9.90	9.00
P_2O_5	2.51	2.11	3.01	2.94	3.12	3.45	2.86	5.44	5.67	5.87	5.99	6.35	5.88	5.87
TiO_2	0.31	0.30	0.29	0.26	0.30	0.32	0.30	0.25	0.26	0.22	0.23	0.21	0.29	0.24
CaO	18.70	19.80	19.50	19.80	18.40	17.10	18.88	29.84	28.90	29.84	26.99	28.12	29.72	28.90
MgO	5.70	6.10	5.10	4.90	5.60	5.70	5.52	1.80	1.75	1.90	1.66	2.10	2.20	1.90
Fe_2O_3	4.51	4.30	4.60	4.90	5.10	5.20	4.77	2.19	2.47	3.10	2.99	2.25	3.21	2.70
Na_2O	0.47	0.41	0.41	0.34	0.44	0.48	0.43	0.25	0.23	0.24	0.22	0.34	0.42	0.28
K_2O	0.91	0.85	0.87	0.81	0.95	0.94	0.89	0.85	0.84	0.88	0.91	0.97	0.99	0.91
SO_3	1.60	1.77	1.80	1.65	1.90	2.10	1.80	3.50	3.60	3.90	3.80	3.10	4.10	3.67
Cl	0.12	0.11	0.11	0.08	0.12	0.11	0.11	0.11	0.11	0.12	0.10	0.12	0.15	0.12
L.I.O	24.96	20.65	23.21	22.52	21.77	19.50	22.10	29.21	30.58	26.73	29.55	26.95	25.15	28.03
Mn	155.00	160.00	181.00	150.00	160.00	156.00	160.33	156.00	180.00	157.00	160.00	180.00	170.00	167.17
Mo	60.00	67.00	70.00	65.00	71.00	75.00	68.00	170.00	185.00	145.00	195.00	187.00	169.00	175.17
Pb	9.50	8.40	9.70	7.90	10.50	10.80	9.47	8.65	8.99	9.25	9.34	8.65	9.11	9.00
Ba	70.00	75.00	80.00	85.00	83.00	90.00	80.50	70.00	75.00	78.00	80.00	85.00	85.00	78.83
Cr	310.00	410.00	350.00	390.00	400.00	370.00	371.67	395.00	380.00	400	415.	450	460.00	416.67
Cu	75.00	97.00	80.00	88.00	90.00	87.00	86.17	88.00	85.00	89	90.	95	101.00	91.33
Co	10.50	13.20	11.20	11.80	12.50	12.10	11.88	5.80	5.10	5.90	6.20	6.70	7.10	6.13
Ni	180.00	195.00	185.00	192.00	193.00	187.00	188.67	265.00	250.00	290	300	355	370.00	305.
Zr	470.00	510.00	490.00	420.00	430.00	550.00	478.33	29.40	33.00	33.50	32.00	40.00	31.00	33.15
V	450.00	490.00	480	470.00	485.00	475.00	475.00	1650	1620	1685	1800	1790.0	1750.00	1715.83
Zn	880.00	850	805	895.00	900.00	910.00	873.33	1180	1205	1250	1420	1450.0	1350.00	1309.17
Rb	35.00	40	33.00	34.00	32.00	33.00	34.50	18.70	18.40	18.90	19.70	21.20	22.50	19.90
Sr	460.00	466	470.00	475.00	472.00	475.00	469.67	620.00	625.00	630.	635	640.00	642.00	632.00
Y	31.00	28	38.00	30.00	33.00	35.00	32.50	23.00	22.00	25.00	29.00	32.00	24.00	25.83
Cd	44.20	40	48.10	44.20	49.20	50.10	45.98	88.00	85.00	95.00	102.00	105.00	99.00	95.67
As	10.20	9.7	11.80	13.00	10.00	15.00	11.62	6.20	7.00	7.50	8.00	9.00	7.80	7.58
Se	18.00	25	19.00	24.00	24.00	20.00	21.67	38.00	40.00	42.00	43.50	44.00	39.00	41.08
Hf	0.95	1.1	1.30	1.20	1.40	1.50	1.24	0.80	0.70	0.88	0.75	0.90	0.85	0.81
Nd	9.70	9.5	11.50	10.00	11.00	12.00	10.62	9.50	10.20	11.00	12.00	14.00	9.20	10.98
Sc	9.20	9.1	8.60	8.70	8.90	10.80	9.22	7.88	6.90	7.10	6.50	8.00	6.10	7.08
Sm	8.50	9.5	11.80	10.00	11.50	12.00	10.55	6.50	7.10	8.50	9.10	9.50	8.60	8.22
La	34.00	31	44.00	35.00	39.00	45.00	38.00	9.10	11.20	12.00	14.00	15.00	8.50	11.63
Ce	40.00	53	48.00	38.00	49.00	51.00	46.50	12.50	15.00	14.00	24.00	25.00	14.90	17.57
Ga	17.00	15	21.00	22.00	25.00	20.00	20.00	9.50	10.00	12.00	14.00	15.00	11.50	12.00
Nb	8.50	9.40	8.80	9.10	8.87	9.10	8.96	4.10	3.90	4.50	4.70	4.90	5.10	4.53
U	31.20	30.40	29.40	34.10	33.50	35.10	32.28	60.20	60.50	64.20	65.10	74.00	70.40	65.73
Th	8.00	5.50	9.70	9.20	10.20	11.00	8.93	2.70	3.80	3.10	3.80	4.10	3.70	3.53
V/Ni	2.50	2.51	2.59	2.45	2.51	2.54	2.52	6.23	6.48	5.81	6.00	5.04	4.73	5.63
Ni/Co	17.14	14.77	16.52	16.27	15.44	15.45	15.88	45.69	49.02	49.15	48.39	52.99	52.11	49.73
V/Mo	7.50	7.31	6.86	7.23	6.83	6.33	6.99	9.71	8.76	11.62	9.23	9.57	10.36	9.80
V/Cr	1.45	1.20	1.37	1.21	1.21	1.28	1.29	4.18	4.26	4.21	4.34	3.98	3.80	4.12
V/(V+Ni)	0.71	0.72	0.72	0.71	0.72	0.72	0.72	0.86	0.87	0.85	0.86	0.83	0.83	0.85
V/(V+Cr)	0.59	0.54	0.58	0.55	0.55	0.56	0.56	0.81	0.81	0.81	0.81	0.80	0.79	0.80
Sr/Ba	6.57	6.21	5.88	5.59	5.69	5.28	5.83	8.86	8.33	8.08	7.94	7.53	7.55	8.02
U/Mo	0.52	0.45	0.42	0.52	0.47	0.47	0.47	0.35	0.33	0.44	0.33	0.40	0.42	0.38
Rb/Sr	0.08	0.09	0.07	0.07	0.07	0.07	0.07	0.03	0.03	0.03	0.03	0.03	0.04	0.03
U/Th	3.90	5.53	3.03	3.71	3.28	3.19	3.61	22.30	15.92	20.71	17.13	18.05	19.03	18.60
Th/U	0.26	0.18	0.33	0.27	0.30	0.31	0.28	0.04	0.06	0.05	0.06	0.06	0.05	0.05
CIA	89.09	90.96	90.23	91.43	89.85	89.27	90.14	86.15	86.17	86.61	87.08	85.46	84.40	85.93
CIW	94.14	95.35	95.01	95.90	94.85	94.27	94.93	94.38	94.63	94.83	95.39	93.45	92.18	94.08
ICV	0.80	0.72	0.73	0.71	0.77	0.81	0.76	0.64	0.68	0.72	0.66	0.62	0.73	0.68
Σtrace	2439.4	2623.4	2470.8	2531.9	2580.2	2667.0	2552.1	3716.1	3679.1	3865.2	4182.5	4309.4	4185	3989.5
ΣTREEs	131.20	140	159.20	130.80	150.27	162.90	145.73	63.08	66.10	71.10	87.30	94.40	67.20	74.86
ΣTLREEs	91.00	102.9	112.60	92.10	108.37	117.10	104.01	32.20	37.20	39.00	51.80	54.40	37.10	41.95
ΣTHREEs	40.20	37.1	46.60	38.70	41.90	45.80	41.72	30.88	28.90	32.10	35.50	40.00	30.10	32.91
ΣLREE/HREEs	2.26	2.77	2.42	2.38	2.59	2.56	2.49	1.04	1.29	1.21	1.46	1.36	1.23	1.27
OM	16.8	16.74	16.98	16.54	17.1	17.5	16.94	18.8	18.9	19.3	19. 1	19.52	18.9	19.08

Table 2: The correlation coefficient for the study black shale samples

	SiO2	Al2O3	P2O5	TiO2	CaO	MgO	Fe2O3	Na2O	K2O	SO3	Cl	L.I.O	Mn	Mo	Pb	Ba	Cr	Cu	Co	Ni	Zr	V	Zn	Rb	Sr	Y	Cd	As	Se	Hf	Nd	Sc	Sm	La	Ce	Ga	Nb	U	Th	Σtrace	ΣTREEs	ΣTLREEs	ΣTHREEs	OM
SiO_2	1.00																																											
Al_2O_3	**0.96**	1.00																																										
P_2O_5	-0.90	-0.95	1.00																																										
TiO_2	**0.72**	**0.74**	-0.76	1.00																																								
CaO	-0.97	-0.97	0.92	-0.74	1.00																																								
MgO	0.96	0.99	-0.97	**0.80**	-0.97	1.00																																						
Fe_2O_3	0.92	**0.94**	-0.87	**0.75**	-0.94	0.92	1.00																																					
Na_2O	0.77	**0.79**	-0.70	**0.83**	-0.76	0.82	0.76	1.00																																				
K_2O	-0.08	-0.09	0.29	0.11	0.07	-0.08	-0.02	0.42	1.00																																				
SO_3	-0.92	-0.94	**0.94**	-0.63	**0.94**	-0.95	-0.84	-0.69	0.22	1.00																																				
Cl	-0.32	-0.26	0.32	0.17	0.34	-0.21	-0.24	0.30	0.74	0.40	1.00																																			
L.I.O	-0.91	-0.91	0.79	-0.70	0.83	-0.88	-0.88	-0.83	-0.12	0.76	0.06	1.00																																		
Mn	-0.36	-0.31	**0.36**	-0.19	0.31	-0.32	-0.40	-0.09	0.22	0.25	0.34	0.31	1.00																																	
Mo	-0.93	-0.96	**0.96**	-0.73	**0.93**	-0.97	-0.93	-0.74	0.20	**0.93**	0.26	0.85	0.40	1.00																																
Pb	0.36	0.27	-0.17	0.49	-0.40	0.32	0.44	0.46	0.52	-0.16	0.30	-0.33	0.00	-0.26	1.00																																
Ba	0.27	0.22	0.06	0.05	-0.21	0.12	0.34	0.32	0.48	-0.05	0.02	-0.47	0.09	-0.07	0.31	1.00																															
Cr	-0.48	-0.44	**0.61**	-0.47	0.58	-0.53	-0.48	-0.28	0.40	0.59	0.33	0.18	0.22	0.60	-0.32	0.42	1.00																														
Cu	-0.28	-0.23	0.38	-0.23	0.40	-0.30	-0.30	-0.09	0.36	0.43	0.35	-0.06	0.09	0.39	-0.29	0.40	0.95	1.00																													
Co	**0.96**	**0.99**	-0.93	0.74	-0.95	0.98	**0.93**	0.79	-0.06	-0.92	-0.25	-0.93	-0.33	-0.94	0.27	0.26	-0.36	-0.14	1.00																												
Ni	-0.82	-0.80	**0.90**	-0.65	0.86	-0.84	-0.79	-0.45	0.49	0.86	0.52	0.59	0.37	0.87	-0.28	0.16	**0.79**	**0.63**	-0.77	1.00																										
Zr	**0.98**	**0.98**	-0.96	**0.78**	-0.98	0.99	**0.93**	0.78	-0.14	-0.95	-0.29	-0.87	-0.30	-0.96	0.34	0.15	-0.58	-0.37	**0.96**	-0.87	1.00																									
V	-0.95	-0.97	**0.98**	-0.76	0.97	-0.98	-0.93	-0.74	0.21	**0.96**	0.33	0.83	0.33	0.98	-0.29	-0.10	**0.62**	0.42	-0.95	**0.91**	-0.99	1.00																							
Zn	-0.88	-0.89	**0.96**	-0.76	0.88	-0.92	-0.85	-0.63	0.38	**0.90**	0.33	0.74	0.30	0.95	-0.24	0.08	**0.69**	0.48	-0.87	**0.94**	-0.93	**0.96**	1.00																						
Rb	**0.92**	**0.98**	-0.97	0.75	-0.93	0.98	**0.88**	0.78	-0.14	-0.93	-0.24	-0.87	-0.30	-0.94	0.14	0.10	-0.45	-0.21	**0.97**	-0.78	0.96	-0.95	-0.88	1.00																					
Sr	-0.95	-0.97	**0.98**	-0.76	**0.97**	-0.98	-0.92	-0.73	0.22	0.97	0.34	0.82	0.34	0.98	-0.28	-0.06	0.63	0.43	-0.95	**0.91**	-0.99	1.00	0.96	-0.95	1.00																				
Y	**0.73**	**0.71**	-0.55	0.37	-0.76	**0.67**	**0.68**	0.62	0.23	-0.70	-0.21	-0.63	0.07	-0.62	0.50	0.45	-0.36	-0.35	**0.68**	-0.49	0.71	-0.66	-0.53	0.61	-0.67	1.00																			
Cd	-0.92	-0.94	**0.99**	-0.77	0.93	-0.96	-0.89	-0.67	0.33	0.94	0.36	**0.78**	0.34	**0.97**	-0.20	0.02	**0.64**	0.43	-0.92	**0.93**	-0.96	**0.99**	**0.98**	-0.94	0.99	-0.55	1.00																		
As	**0.88**	**0.81**	-0.67	0.55	-0.85	0.77	**0.84**	**0.67**	0.01	-0.76	-0.38	-0.81	-0.24	-0.75	0.36	0.58	-0.39	-0.27	**0.79**	-0.63	**0.83**	-0.79	-0.67	0.74	-0.77	**0.79**	-0.72	1.00																
Se	-0.92	-0.93	**0.95**	-0.83	0.94	-0.95	-0.91	-0.79	0.16	0.92	0.23	**0.79**	0.29	0.96	-0.36	-0.05	0.69	0.50	-0.90	**0.88**	-0.97	**0.98**	**0.95**	-0.91	0.97	-0.66	**0.96**	-0.78	1.00															
Hf	0.91	0.85	-0.72	0.63	-0.85	**0.82**	**0.88**	0.73	0.09	-0.76	-0.20	-0.90	-0.22	-0.81	0.54	**0.53**	-0.30	-0.15	**0.87**	-0.67	**0.85**	-0.83	-0.75	0.74	-0.81	**0.78**	-0.75	**0.86**	-0.79	1.00														
Nd	0.01	-0.11	0.31	-0.43	0.00	-0.15	-0.12	-0.07	0.40	0.05	-0.11	0.04	0.37	0.23	0.29	**0.51**	0.20	0.02	-0.11	0.24	-0.10	0.18	0.33	-0.20	0.17	**0.54**	0.29	0.23	0.22	0.17	1.00													
Sc	**0.93**	**0.81**	-0.77	**0.61**	-0.86	**0.85**	**0.74**	0.68	-0.07	-0.84	-0.32	-0.77	-0.34	-0.80	0.38	0.18	-0.54	-0.37	**0.80**	-0.77	**0.87**	-0.84	-0.78	0.77	-0.84	**0.67**	-0.80	**0.80**	-0.82	**0.81**	0.12	1.00												
Sm	**0.76**	**0.74**	-0.54	0.45	-0.76	0.68	**0.79**	0.65	0.28	-0.62	-0.14	-0.79	0.01	-0.63	0.56	**0.68**	-0.14	-0.07	**0.75**	-0.45	**0.72**	-0.66	-0.53	0.63	-0.65	**0.90**	-0.55	**0.83**	-0.62	**0.90**	0.44	0.61	1.00											
La	**0.95**	**0.94**	-0.87	**0.69**	-0.97	**0.93**	**0.93**	0.74	-0.07	-0.92	-0.33	-0.83	-0.20	-0.91	0.46	0.29	-0.58	-0.43	**0.91**	-0.84	**0.96**	-0.95	-0.88	0.87	-0.94	**0.84**	-0.90	**0.89**	-0.93	**0.91**	0.10	0.85	0.84	1.00										
Ce	**0.95**	**0.96**	-0.89	**0.69**	-0.96	**0.95**	**0.88**	0.75	-0.01	-0.91	-0.27	-0.86	-0.18	-0.87	0.38	0.25	-0.42	-0.23	**0.96**	-0.78	**0.96**	-0.92	-0.83	0.93	-0.93	**0.79**	-0.88	**0.80**	-0.87	**0.86**	0.10	0.83	0.81	0.94	1.00									
Ga	**0.81**	**0.84**	-0.70	**0.47**	-0.86	**0.78**	**0.87**	0.63	0.08	-0.80	-0.32	-0.74	-0.20	-0.77	0.42	0.48	-0.32	-0.27	**0.82**	-0.64	**0.79**	-0.80	-0.68	0.71	-0.80	**0.83**	-0.72	**0.80**	-0.75	**0.88**	0.23	0.66	0.87	0.89	0.82	1.00							
Nb	**0.97**	1.00	-0.95	**0.74**	-0.97	**0.98**	**0.95**	0.79	-0.09	-0.94	-0.28	-0.91	-0.32	-0.96	0.27	0.24	-0.46	-0.25	**0.99**	-0.80	**0.98**	-0.97	-0.89	0.98	-0.97	**0.71**	-0.94	**0.83**	-0.93	**0.86**	-0.10	0.81	0.75	0.94	0.95	0.84	1.00						
U	-0.91	-0.94	**0.98**	-0.75	**0.94**	-0.95	-0.89	-0.65	0.33	**0.94**	0.38	0.76	0.34	**0.96**	-0.27	0.03	**0.68**	0.48	-0.91	0.95	-0.96	**0.98**	**0.98**	-0.92	**0.99**	-0.60	**0.99**	-0.71	**0.96**	-0.76	0.25	-0.79	-0.59	-0.92	-0.89	-0.74	-0.94	1.00					
Th	**0.90**	**0.88**	-0.78	**0.68**	-0.93	**0.86**	**0.93**	**0.73**	0.03	-0.84	-0.29	-0.79	-0.20	-0.85	0.53	0.42	-0.53	-0.42	**0.85**	-0.77	**0.89**	-0.89	-0.80	**0.77**	-0.88	**0.81**	-0.83	**0.90**	-0.89	**0.92**	0.11	**0.80**	**0.84**	**0.96**	**0.86**	**0.93**	0.88	-0.84	1.00				
Σtrace	-0.90	-0.92	**0.97**	-0.75	**0.93**	-0.94	-0.89	-0.65	0.33	0.94	0.37	**0.75**	0.34	**0.97**	-0.26	0.03	**0.71**	0.52	-0.89	0.95	-0.95	**0.98**	**0.99**	-0.90	0.98	-0.58	**0.99**	-0.72	**0.97**	-0.77	0.26	-0.80	-0.56	-0.91	-0.86	-0.74	-0.92	**0.99**	-0.85	1.00			
ΣTREE	**0.94**	**0.94**	-0.83	**0.61**	-0.95	**0.91**	**0.89**	**0.74**	0.04	-0.89	-0.31	-0.86	-0.16	-0.85	0.42	0.38	-0.39	-0.25	**0.93**	-0.73	**0.93**	-0.89	-0.78	**0.88**	-0.90	**0.88**	-0.83	**0.86**	-0.84	**0.90**	0.23	**0.82**	**0.89**	**0.96**	**0.98**	**0.90**	**0.94**	-0.85	**0.91**	-0.82	1.00		
ΣTLREE	**0.95**	**0.95**	-0.85	**0.65**	-0.97	**0.93**	**0.91**	**0.74**	0.01	-0.91	-0.31	-0.85	-0.18	-0.88	0.45	0.35	-0.46	-0.31	**0.94**	-0.78	**0.95**	-0.92	-0.82	**0.88**	-0.92	**0.87**	-0.86	**0.87**	-0.88	**0.92**	0.17	**0.83**	**0.88**	**0.98**	**0.98**	**0.91**	**0.95**	-0.88	**0.94**	-0.86	**0.99**	1.00	
ΣTHREE	**0.82**	**0.77**	-0.63	0.45	-0.83	**0.75**	**0.74**	**0.67**	0.18	-0.78	-0.25	-0.70	-0.02	-0.70	0.50	0.42	-0.42	-0.37	**0.75**	-0.59	**0.79**	-0.74	-0.62	**0.69**	-0.74	**0.99**	-0.64	**0.84**	-0.74	**0.84**	0.48	**0.78**	**0.89**	**0.90**	**0.85**	**0.85**	**0.78**	-0.68	**0.86**	-0.67	**0.92**	**0.91**	1.00	
OM	-0.88	-0.95	**0.98**	-0.75	**0.92**	-0.94	-0.89	-0.68	0.31	**0.94**	0.37	**0.76**	0.36	**0.95**	-0.12	0.00	**0.59**	0.38	-0.92	**0.88**	-0.94	**0.97**	**0.95**	-0.95	**0.97**	-0.55	**0.98**	-0.70	**0.95**	-0.71	0.34	-0.72	-0.54	-0.87	-0.86	-0.74	-0.95	**0.97**	-0.81	**0.97**	-0.81	-0.84	-0.62	1.00

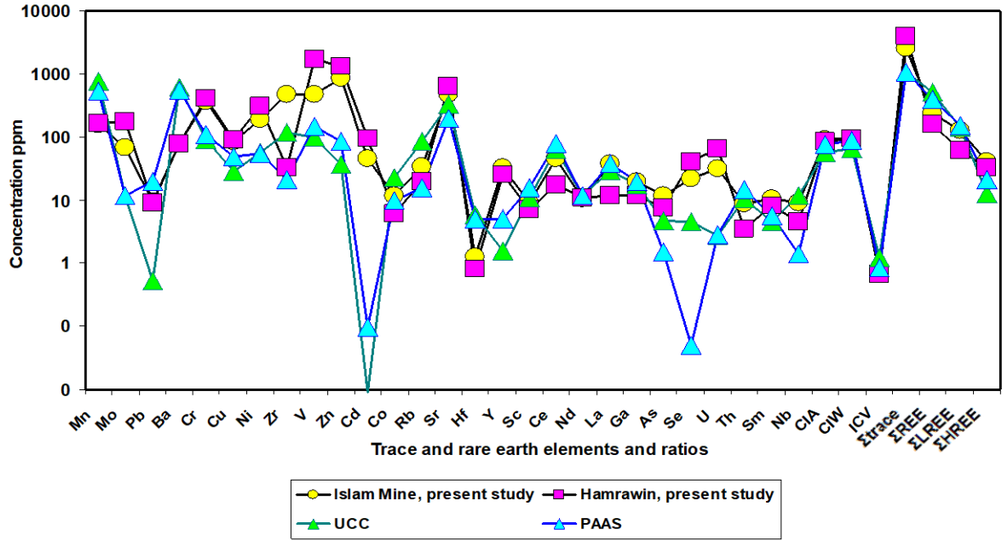

Fig. 5: The spider diagram for the traces and rare earths elements of the investigated samples normalized to the average UCC and PAAS [25, 26]

Islam mines recorded high concentration in the total traces than those of the Hamrawin mines (average 3989.52 and 2552.12ppm; respectively). Thus, Islam mines higher concentration than Hamrawin mines, consequently, there is an increase in the traces to the south. In contrast, Hamrawin mines recorded high values in the ΣREEs, ΣLREEs (La, Ce, Sm and Nb) and ΣHREEs (Y and Sc), (average 145.73, 104.01 and 41.72ppm; respectively) than those recorded in the Islam samples (average 74.86, 41.95 and 32.91ppm; respectively) (Fig. 6). Thus, the trace elements increased from central to south direction whereas rare earths decreased for Qussier area.

Mo, Ni, V, Zn, Cr, and Cd are strongly positively correlated with P_2O_3 (r = 0.96, 0.90, 0.98, 0.96, 0.61 and 0.94; respectively) and both rare earth elements Se and U (r= 0.95 and 0.98; respectively). Thus, these elements were coupled with apatite minerals. SO_3 strongly positive correlated with OM, V, Zn, Cd and Se (r= 0.94, 0.96, 0.90, 0.92 and 0.94; respectively), therefore these elements may also be associated with sulphides minerals (Table 2). Thus, the traces and most rare earths are enriched in organic-rich sediments which agree with [35, 14]. Strongly positive correlation between P_2O_3 and OM (r =0.98), revealed detrital phosphate minerals were occurred.

Co, Zr, and Rb and the rare earths; Y, As, Hf, Sc, Sm, La, Ce, Ga, Nb and Th are strongly positive correlated with Al_2O_3 (r= 0.99, 0.98, 0.98, 0.71, 0.81, 0.85, 0.81, 0.74, 0.94, 0.96, 0.84, 1 and 0.88; respectively), with SiO_2 (r= 0.96, 0.98, 0.92, 0.73, 0.88, 0.91, 0.93, 0.76. 0.95, 0.95, 0.81, 0.97 and 0.90; respectively) and with Fe_2O_3 (r= 0.93, 0.93, 0.88, 0.68, 0.84, 0.88, 0.74, 0.79, 0.93, 0.88, 0.87, 0.95 and 0.93; respectively), as well as Mg (r= 0.98, 0.99, 0.98, 0.67, 0.77, 0.82, 0.85, 0.68, 0.93, 0.95, 0.78, 0.98 and 0.86; respectively). Thus these elements are associated with clay minerals and ferromagnesian oxides and/or the detrital materials (Table 2).

Generally, no correlation was recorded between Σtraces with Al_2O_3 and SiO_2, but strong positive correlations were recorded with P_2O_3, CaO and OM (r=0.97, 0.93 and 0.97; respectively). This suggests that Σtraces were enriched in the phosphate minerals and the OM of the studied

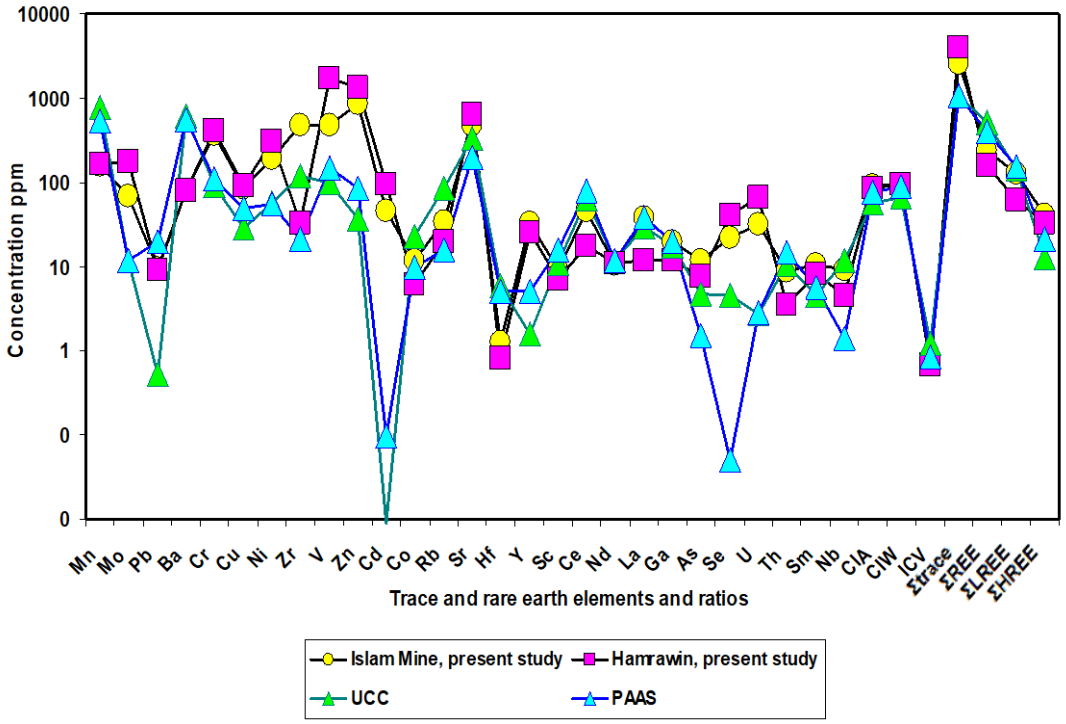

Fig. 5: The spider diagram for the traces and rare earths elements of the investigated samples normalized to the average UCC and PAAS [25, 26].

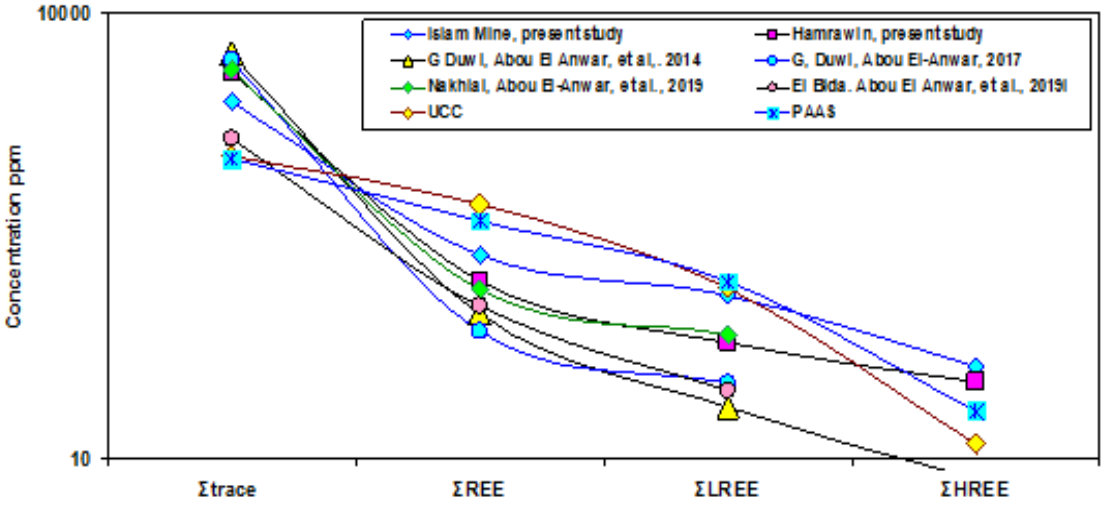

Fig. 6: Distribution of traces, ΣREEs, ΣLREEs, ΣHREEs for the study area and others localities**.**

samples. In contrast, there are strong positive correlations between ΣREEs with SiO_2, Al_2O_3, TiO_2, MgO and Fe_2O_3(r=0.94, 0.94, 0.91 and 0.89; respectively), which indicated that the most REEs were associated with clay minerals and ferromagnesian oxides and/or the detrital materials. Also, the strong negative correlation with OM (r=-0.81) was supported it. The same vision is noticed for ΣLREEs and ΣHREEs.

3.2.3. Distribution of Uranium and Thorium

U content in the study samples ranges from 29.4 to 74 ppm for Islam and Hamrawin mines; respectively (Table 1). The average values for both Islam and Hamrawin black shales samples are 32.28 and 65.73 ppm; respectively. These values are higher than U value in the UCC (2.5ppm) and the PAAS (2.7ppm). Therefore, the study samples can be recognized as uraniferous black shales [36]. In marine black shales U was derived from sea water. U could have been accumulated in hydrogen sulfide condition [36]. Thus, high positive correlation between SO_3 and U (r = 0.94) and the abundance of pyrite in the studied black shales, reveal that this elevated U contents concentrated in black shales beneath a hydrogen sulfide condition and regularly increased under diagenetic processes [36]. Also, this high concentration of U may be attributed to the post-depositional enrichment of uranium and/or intensive chemical weathering in Qussier area [15].

U is concentrated under reducing conditions resulting of the preservation of the organic matter. So, U can be considered as a good indicator of organic matter. U > 5 ppm is usually represented as cut-off for black shale [37]. U has a strong positive correlation with P_2O_5, CaO and Sr (r= 0.98, 0.94 and 0.99; respectively) as well as OM (r= 0.98). Hence, it indicates that U was best associated with these elements in phosphate minerals and organic matter. In addition to, it pointed out that the vital role of phosphate in fixation of $U6^+$ as uranyle ion $(UO_2)^{2+}$. Thus, the secondary uranium minerals can be accumulated during subaerial weathering [36].

U is strong positive correlated with Mo, Ni, V, Zn, Cd, Cr, Cu and Se (r= 0.96, 0.95, 0.98, 0.98, 0.99, 0.68, 0.48 and 0.96; respectively). Therefore, U may be released during the weathering and act as immobile [38]. Thus, U contents in the study black shales were probably associated with the heavy metals and some rare earths up on the chemical weathering [38, 39, 40], under oxic environment [41]. Generally, anoxic sediments are mostly extra enriched in U than oxic sediments [42, 16, 43, 44, 45].

Th content varies from 2.7ppm (recorded in Hamrawin black shales samples) to 11ppm (recorded in Islam black shales samples) with averaging 8.93 and 3.53 ppm in Islam and Hamrawin black shales samples; respectively. These values are lower than those recorded in UCC and PAAS (10.3 and10.5ppm; respectively), Fig. (5). Consequently, Th content increased from north (Safaga) to south (Qussier) which is conformed by Abou El-Anwar, et al., [46].

Th recorded strong positive correlation (r= 0.90, 0.88, 0.68, 0.86, 0.93 and 0.73; respectively) with SiO_2, Al_2O_3, TiO_2, MgO, Fe_2O_3 and Na_2O indicated that the Th content is mostly associated with clay minerals and ferromagnesum minerals. Th is strong positive correlated (r= 0.89 and 0.85; respectively) with the traces Zr and Co, in addition with most rare earths; Rb, Y, As, Hf, Sc, Sm, La, Ce, Ga and Nb (r= 0.77, 0.81, 0.90, 0.92, 0.80, 0.84, 0.96, 0.86, 0.93 and 0.88; respectively). Also, Zr is strong positive correlated (r= 0.96, 0.71, 0.83, 0.85. 0.87, 0.72, 0.96, 0.96, 0.79 and 0.98; respectively) with the same rare earths. Thus, Th possibly associated with zirconium mineral.

3.2.4. Depositional environment and paleo-redox elements

The geochemical results of the studied shale can be used to inspect their probably depositional setting of Duwi Formation. V, P, and Al contents are used to recognize the depositional setting of the studied samples. V contented was usually higher for a marine sedimentary rock as well as P content substantially fluctuates in seawater. V and Al_2O_3 binary diagram (Fig. 7) revealed that the studied black shale samples are plotted in the shallow marine setting field [48]. Also, P_2O_5 and Al_2O_3 binary diagram (Fig. 8) conformed to the same interpretation of Fig. (7). The studied black shales contain high concentrations of Cr and Ni (average 393 and 250 ppm; respectively) indicated these black shales were deposited under shallow marine conditions [47]. U/Mo ratio (0.40) indicates the black shales of the studied area were deposited under an anoxic sulphidic marine environment [20, 13, 11]. Thus, Figs. 7 and 8 revealed that the Hamraw in shales were deposited in more deep places than those of Islam mine.

Some of the geochemical parameters can be utilized to evaluate the marine paleoredox conditions of sediments, such as redox-sensitive traces; V, Ni, Cr, Re, Mo, U, Cu, Cd, Se, Tl and Sb, as well as ratios of traces; Th/U, Ni/Co, V/Mo, V/Ni, V/(V + Ni) and V/(V + Cr), and the depletion content of Mn. The high contents of these redox-sensitive traces refer to anoxic conditions in sediments [49, 12, 18, 16, 43, 46].

V, Mo, Zn, Cr, Zr, Cd, Sr, and rare earths; Y, As, Se, Sm and U in the studied area are higher than those of (UCC) and (PAAS), and Pb is lower than PAAS and higher than UCC (Table 1 and Fig. 5). While Mn, Ba, Pb, Co, Rb, Hf, Sc, Ce, Nd, La, Nb and Th were lower than those of (UCC) and/or (PAAS) as well as low content of Mn (~164ppm). Thus, the content of these traces, REES and Mn indicated the studied black shales were deposited

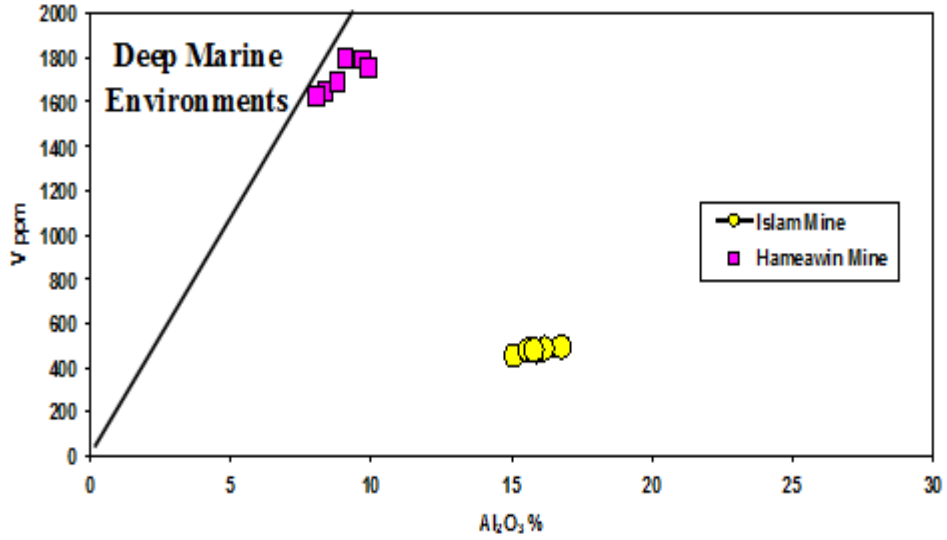

Fig. 7: The V_{ppm}-Al_2O_3% bivariate diagram plot for the study samples in shallow marine environment, after [48].

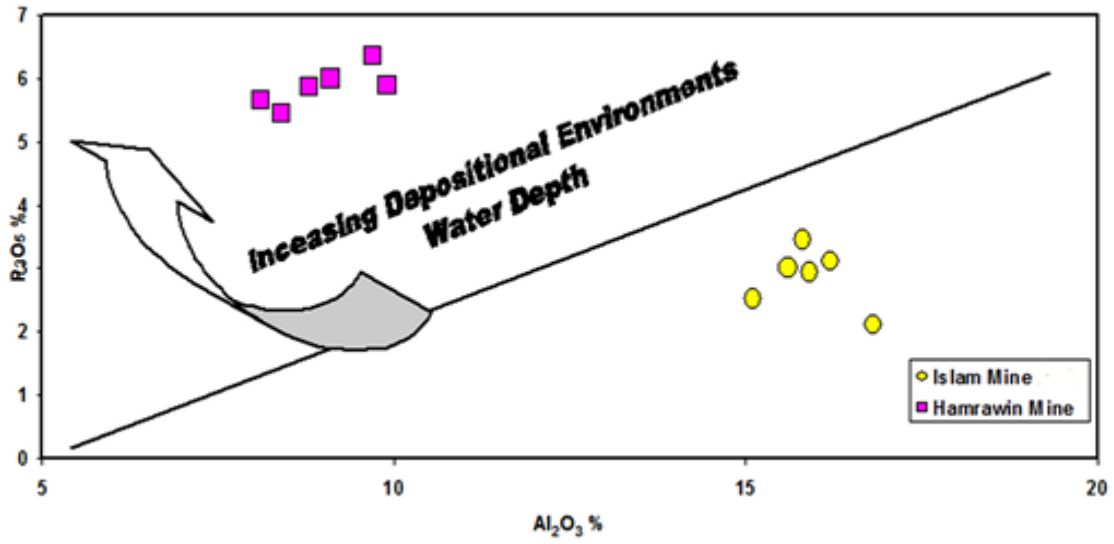

Fig. 8: P_2O_5- Al_2O_3 % bivariate diagram plot for the study samples, after [48]

during anoxic conditions. Therefore, these elements can be used as paleo-redox indices [50].

The studied black shale samples have V/(V + Ni) > 0.8 (average 0.81), V/Ni (average 4.39), Ni/Co (average 27.74) and Th/U (average 0.13), these suggest strong anoxic conditions [51, 52, 53, 54]. High strong positive correlation (r= 0.88 and 0.95; respectively) between Ce and Fe and Mg revealed that the Ce^{4+} is, most probably, adsorbed on oxy-hydroxides of Fe and Mg of the oceans, which may explain the positive Ce anomaly, which indicated the studied black shale samples were deposited under anoxic conditions [55, 56].

While V/(V + Cr) (average 0.74), V/Mo (average 2.94) suggest suboxic conditions. The discrepancy between the depositional environments anoxic to suboxic environments was possibly resulting of the mobility of these metals during diagenesis and/or weathering. Also, high contents of OM (average 18.02 %) has been interpreted anoxic depositional condition [57]

3.2.5. Source of traces and rare earths

The traces and rare earths may be originated from marine sedimentary rocks [58], seawater, organic matter [59] or hydrothermal solutions [31].

The studied samples showed a strong positive correlation off organic matter with most traces and rare earths, revealing that these elements likely originated from marine organic sources. The high enrichments of certain traces, V, Cr, Ni, As, Sr, Mo, and Cd, may be related to hydrothermal activity. The abundances of V, Zn, Cr, Ni, Mo, Cd, As are much higher than those of PAAS and UCC, can be indicated to hydrothermal or hydrogenous or biogenic origin [59, 31]. The positive correlation between SiO_2 and Al_2O_3 with rare earths Y, AS, Hf, Sc, Sm, La, Ce, Ga, Nb and Th suggests detrital input. Thus, the black shales for the Duwi Formation in the Qussier area had diverse sources for redox-sensitive traces and rare earths.

The Zr ppm vs TiO_2 % bivariate discrimination diagram according to McLennan, et al., [60] indicated that the study Islam mine black shales samples are plotted in the felsic filed and Hamraw in mine samples plotted in mafic field (Fig. 9).

Also, the high Fe_2O_3 content, some traces and REEs; Zr, V, Sr, Th, Y, Hf, concentrations possibly resulted from the recycling and enrichment from the underlying rocks.

3.2.6. Mobilization of Rare Earths (REEs)

REEs are mainly originated from rock and mineral weathering, erosion and soil parent material [61]. Concentrations of REEs naturally found in sediments depend on the parent material.

LREE recorded 125.67 and 52.7ppm as average in the studied samples from Islam and Hamrawin mines; respectively, and HREE recorded 41.72 and 30.1ppm as average; respectively for the same mines (Table1). Thus, the enrichment of LREEs and depletion of HREEs, were resulting of the weathering process.

LREE/HREE ratios (3.01 and 1.75 for Islam and Hamraw in mines; respectively) revealed that weathering processes had extra affected on REE fractionation in Islam mine than Hamrawin mine. LREEs low mobility compared with HREEs led to the LREEs enrichment, whereas HREEs depletion coupled with raise weathering intensity in sediments derived from metaluminous granites [62, 63].

LREEs (La, Ce, Ga, Nd and Sm) are mainly strong positive correlated with SiO_2 (r= 0.95, 0.95, 0.81, 0.97 and 0.74; respectively) and Al_2O_3 (r=0.94, 0.95, 0.84, 1 and 0.74), which indicated that the LREEs are associated with clay minerals and/or quartz grains. Also, HREE; Y and Sc have strong positive relation with SiO2 (r= 0.73 and 0.93; respectively) and Al_2O_3 (r= 0.71 and 0.81; respectively) which revealed that the HREEs are associated with detrital materials. Generally, REEs have least mobility within near-surface environments. Consequently, these elements those reflect nearby sources.

3.2.7. Alteration and chemical weathering effect

The chemical composition of weathering products is probable give an idea on mobility of a variety of elements during weathering. During chemical weathering, Ca, Na and K are mainly removed from source rocks and Al is the least mobile element. Thus, chemical index of alteration (CIA) which was proposed with Nesbitt and Young,) [64] can indicate the intensity of weathering in source areas.

$$\mathbf{CIA = [Al_2O_3/(Al_2O_3 + CaO^* + Na_2O + K_2O)] \times 100;}$$

CaO* represents CaO associated with the silicate fraction of the sample.

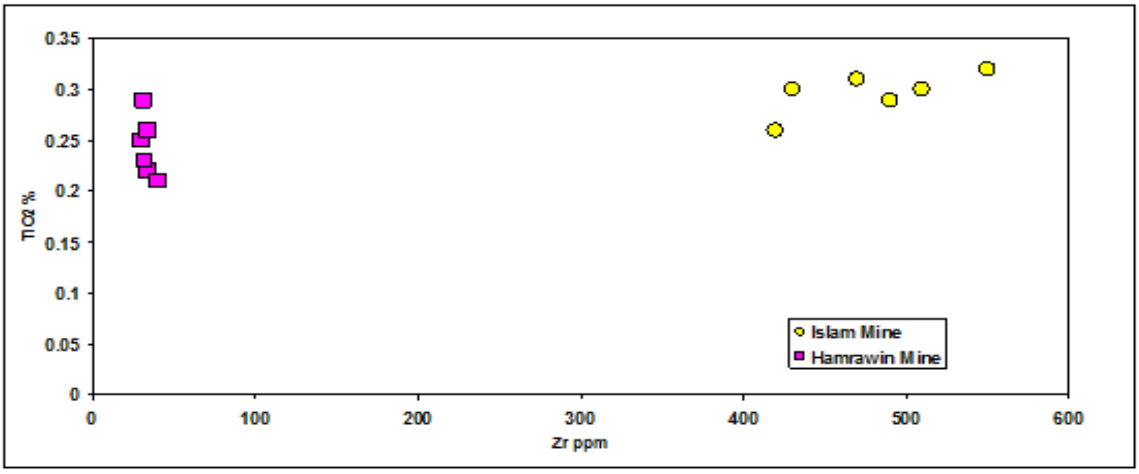

Fig. 9: The Zr $_{ppm}$–TiO_2 % discrimination plot for the study samples after [60]

The CIA values in the studied samples range from 84.4 (Hamrawin mine) to 90.43% (Islam mine), averaging 88.04% for all the study area (Table 1). This average indicates that the basis of the primary minerals was derivative from felsic (Islam mine) to mafic (Hamrawin mine) origins and, generally, subjected to extremely intensive chemical weathering [64, 65]. In addition, the samples of the Islam mine are subjected to more intensive chemical weathering than those of Hamrawin samples.

The chemical index of weathering (CIW) ranges from 92.18% (Hamrawin mine) to 95.9% for Islam mine, with averaging 94.47% for the study area, which indicated that black shales samples were subjected to intensive chemical weathering either of the original source or during transportation before deposition.

The immobile elements are useful indicators of provenance of weathering [25]. Thus, the strong positive correlations off Al_2O_3 with Ti, Co, Zr, Y, Sc, Ga, Sm and Th) r= 0.74, 0.99, 0.98, 0.71, 0.81, 0.84, 0.74 and 0.88; respectively (Table 2) reveal that these elements are accumulated during chemical weathering processes. Thus, the study area was subjected to chemical weathering condition [66, 14].

Rb/Sr ratios can be recognizing the degree of weathering for the source rock [67]. The studied black shale samples have an average Rb/Sr ratio of 0.05 (Table 1). It is lower than that of average of the UCC and PAAS (0.33 and 0.08; respectively). Thus, it indicated that the degree of the chemical

weathering of the source study black shales was relatively comparable to the PAAS values.

3.2.8. Maturation

The most common system to identifying the degree of sedimentary recycling is to estimate the maturity of the composition. The Index of the Compositional Variability (ICV) was as a parameter to measure the compositional maturity degree [68]:

$$ICV = (Fe_2O_3 + K_2O + Na_2O + CaO + MgO + MnO)/ Al_2O_3$$

ICV < 1 are characteristic of kaolinite, illite and muscovite and (>1) are indicated to plagioclase, K-feldspar, amphiboles and pyroxenes rocks [68]. Also, the more mature shales with mostly clay minerals must to record low ICV values (<1.0), and are subjected to high intensity of chemical weathering and predominate recycling processes [69]. The ICV values of the investigated shales of Duwi Formation range from 0.62 (Hamrawin samples) to 0.81(Islam samples), average (0.72), Table (1). Thus, the studied black shales of in Hamrawin and Islam mines are subjected a highly weathering and more maturation. Also, it indicates the dominance of kaolinite in the study samples, which is supported by the mineralogical analysis (Fig. 3). As well as the ICV average (0.72) was lower than those of the PAAS and UCC values (0.85 and 1.2; respectively). It is revealed that the studied black shales are compositionally highly mature. Also, high percentages of organic matter (averaging 18.02 %) revealed that these black can be classified as high-quality sources for extraction oil and gas.

3.2.9. Paleosalinity

The Sr/Ba ratio was applied to define the difference in water salinity and its corresponding climatic environment [70, 71]. Also, they mentioned that the high Sr/Ba ratio is represented the high salinity and arid hot climate conditions, whereas a low ratio pointed out to low salinity and a humid warm climate [70, 71]. Sr/Ba for the studied black shale samples are ranges from (5.87 for Islam mine) to (7.53 for Hamrawin mine) with averaging 6.91 for the study area, which indicating a hot climatic condition. The Sr/Ba versus V/Ni ratio plot (Fig. 10) is confirmed the result of Sr/Ba ratios [49], where the studied samples are plot in the high salinity fields. This climate a condition is also supported by the (CIA) values (from 84.4 to 90.43%) for the Duwi black shales.

3.2.10. Tectonic setting

Generally, the geochemical and mineralogical compositions of marine sediments are related to their tectonic settings [72, 73].

The tectonic settings based on SiO_2 content and K_2O/Na_2O ratios were proposed by Roser and Korsch [74]. The binary diagram has been divided into three categories. Plotting of the samples under study in the binary diagram log K_2O/Na_2O - SiO_2 shows that all the black shale samples of Duwi Formation fall in the active continental margin of provenance (Fig. 11). The high matured sediments are derived by recycling of older sedimentary and metamorphic rocks of platforms [75]. Thus, the investigated black shalesrelated to the active continental margin of provenance and may be original by recycling of older sedimentary and metamorphic rocks.

3.2.11. Paleoclimate

The highly in the degree of chemical weathering may indicate a decrease in tectonic activity and/or change in climate towards warm and humid conditions [76]. Paleoclimate is a most factor in the evaluation of the composition and weathering of sedimentary rocks [77]. Thus, the paleoclimate was represented a main parameter to be identified the evaluation of the composition and weathering of sedimentary rocks.

Several proxies such as clay composition as well as trace element contents and ratios (Sr/Cu and Sr/Ba ratios), have been widely used to examine paleoclimatic conditions.

The Sr/Cu ratio is an important indicator of paleoclimate, where Sr/Cu ratio >5, indicated to a hot-arid climate, and Sr/Cu from 1.3 to 5.0 indicates warm and humid climate conditions (Ben-Awuah, et al., 2017). The Sr/Cu ratios of the studied black shale vary from 4.8 for Islam mine to 6.35 (for Hamrawin mine) with averaging 5.74 for all samples of the study area. The diagram shows warm and cool climate condition and Sr/Cu ratio >5, so according to Ben-Awuah, et al., [79]. Plotting of the studied samples in the binary diagram Sr/Cu – Ga/Rb shows that the climate of black shale samples of Duwi Formation was hot arid (Fig. 12), [78].

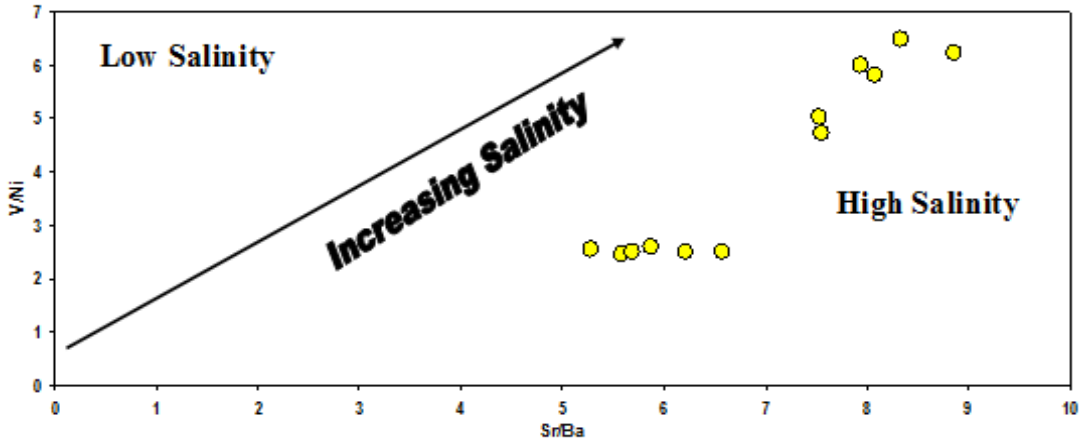

Fig. 10:Sr/Ba ve. V/Ni bivariate diagram for the Duwi shale samples [49].

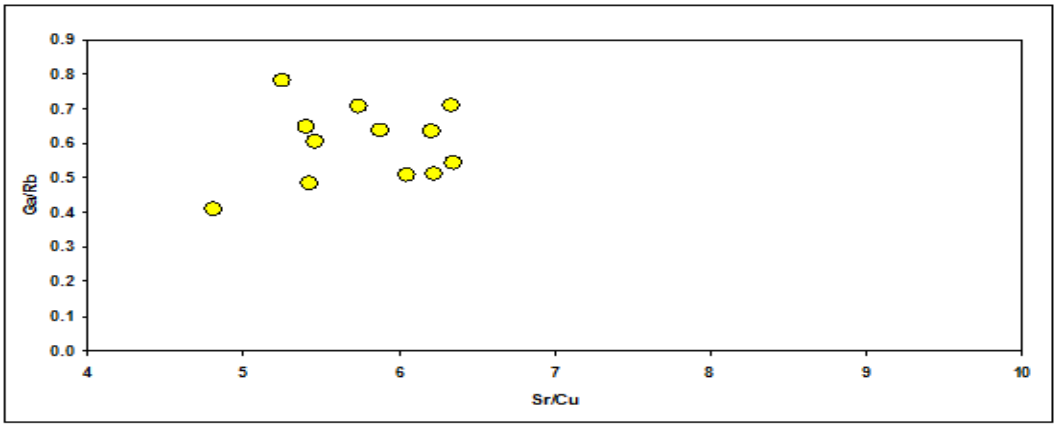

Fig. 11: Tectonic setting discrimination plots SiO2 and (K2O/Na2O) for the study samples [74].

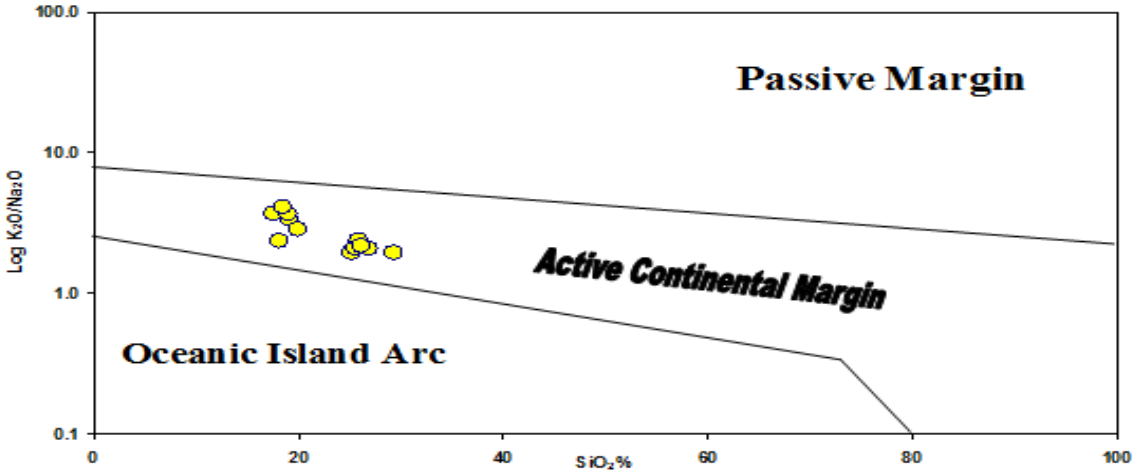

Fig. 12: Sr/Cu vs. Ga/Rb binary diagram for the study shale samples [78].

The high average CIW value (94.47%, Table 1) indicated that intense recycling in a humid climate or intense recycling in hot/arid climate [81].

3.3. Comparison of the chemical composition with other localities:

Table (3) shows the distribution of the traces, Σtraces, CIA, ICV and CIW in the study black shales and in some other mines; Gebel Duwi mines, Gebel El-Nakhial and El-Bida as well as UCC and PAAS contents. Table (4) shows the concentration of the REEs, ΣREEs, ΣLREEs and ΣHREEs.

Generally, the study black shales in Islam and Hamrawin mines are enrichment than those recorded in UCC and PAAS vales. The black shale samples Hamrawin are enhancement in V average than all the other mines (Table 3 and Fig. 13). In addition the low concentration of it was recorded in Islam mines, thus, V concentration decreases from Hamrawin mine in from central to south of Qussier.

But, Islam mines black shale was recorded the highest value of CIA and CIW (90.14 and 94.93%; respectively), thus the chemical weathering increased to the south direction of Qussier. Gebel Duwi mines (Abou El-Anwar, et al., 2017) [24].represented the highest maturity (ICV= 0.92%).

GebleDuwi black shales are enrichment in Mn, Cr and Cu, as well as recorded the highest average of Σtraces [13]. In addition, (Abou El-Anwar, et al.,) [14] recorded the high enrichment in averages Ni, Zr, Cd and Sr. the high enrichment of Mn, Mo, Ba, Zn, Co and As are recorded in Gebel El-Nakhial samples [14]. However, the highest concentration of Pb for Gebel El-Nakhial black shale samples was determined with Abou El-Anwar, et al., [14].

The study of black shale samples in Islam mines are represented the highest content of Hf, Y, Sc, Ce, La, Rb, Sm and Th (1.24, 32.5, 9.22, 38, 34.5,10.55 and 8.93ppm; respectively) from all the other mines (Table 4 and Fig. 14). Generally the black shales of Islam mines are represented the highest average of ΣREEs, ΣLREEs and ΣHREEs (233.75, 125.67 and 41.72ppm; respectively) than all the other mines. Consequently, the ΣREEs are increased to the direction of south Qussier.

4. Conclusions

The black shales in the Qusseir area (Duwi Formation) were deposited in an anoxic shallow marine environment. Highly enrichment of redox-sensitive elements of the studied marine black shales can be considered as strong verification for anoxic conditions existing during the deposition of the shales of the Qusseir area of the Duwi Formation. XRD analyses indicated the studied black shales are consisted of two phases, clay and non clay minerals. The chemical analyses indicated that it was deposited under high salinity, hot arid climate conditions. Also, the chemical analyses revealed the study black shales are more mature and subjected to intensity chemical weathering.

The high some traces and REEs minerals revealed to input of recycling components derived from old sedimentary source in a comparatively stable tectonic setting [82, 14]. Resulting of the high contents of some traces and REEs minerals indicated that the studied black shales have economic values for industry; wind power, linear fluorescent lamps, compact fluorescent lamps, light-emitting diode, electric vehicles, electric bicycles, batteries, and catalytic converter. Generally, the ΣREEs are increased in direction from central to south Qussier.

4. Conflicts of interest

"There are no conflicts to declare".

5. Formatting of funding sources

Not applicable

6. Acknowledgments

Many thanks to National Research Centre for logistic and lab facilities.

Table 3: Traces elements, CIA, CIW and ICV of the black shale for this study as compared with published average in different localities.

	Islam Mine, present study	Hamrawin Mine, present study	G Duwi, Abou El Anwar, et al., 2014, [13]	G, Duwi, Abou El-Anwar, 2017, [16]	Nakhial, Abou El-Anwar, et al., 2019, [14]	El Bida, Abou El Anwar, et al., 2019, [14]	UCC	PAAS
Mn	160.33	167.17	**390**	154.9	**390.2**	309.5	770	539
Mo	68	175.17	511.75	110	**591.6**	148.5	12	12
Pb	9.47	9	11.25	11	38.9	**63.5**	0.52	20
Ba	80.5	78.83	79	0	**189.7**	83.25	624	550
Cr	371.67	416.67	**1107.75**	752.6	961.7	349.25	92	110
Cu	86.17	91.33	**235.25**	214.5	222	46	28	50
Ni	188.67	305	245.5	**393.1**	230.1	96.5	57	55
Zr	478.33	33.15	47.5	**740.3**	71.1	123.25	120	21
V	475	**1715.83**	1693.75	1232.4	1314.1	533.25	97	150
Zn	873.33	1309.17	1959.5	1205.09	**1378.5**	192	37	85
Cd	45.98	95.67	7.25	**290**	155.3	7.25	0.009	0.098
Co	11.88	6.13	0	0	**52.6**	0	23	10
Sr	469.67	632	**510**	**676.5**	155.3	7.25	336	200
As	11.62	7.58	29	17	**67.8**	29	4.8	1.5
CIA	**90.14**	85.93	85.03	88.16	87.62	85.03	56.93	75.3
CIW	**94.93**	94.08	94.3	95.32	89.4	94.3	65.24	88.32
ICV	0.76	0.68	0.71	**0.92**	0.87	0.71	1.2	0.85
Σtraces	2552.12	3989.53	**5336.75**	4838.99	4128.17	1440	1078.2	1051

Table 4: The REEs the black shels in this study as compared with published average in different localities

	Islam Mine, present study	Hamrawin Mine, present study	G Duwi, Abou El Anwar, et al., 2014, [13]	G, Duwi, Abou El-Anwar, 2017, [16]	Nakhial, Abou El-Anwar, et al., 2019, [14]	El Bida, Abou El Anwar, et al., 2019, [14]	UCC	PAAS
Hf	**1.24**	0.81	0	0	0	0	5.8	5
Y	**32.5**	25.83	7.25	30	7.85	13.75	1.6	5
Sc	**9.22**	7.08	0	0	0	0	11	16
Ce	**46.5**	17.75	0	0	0	0	64	80
Nd	10.62	**10.98**	0	0	0	0	12	12
La	**38**	11.63	0	0	0	0	30	38
Ga	20	12	22.5	0	**23.5**	22.5	17.5	20
Rb	**34.5**	19.9	26.5	29	14.7	26.5	84	16
Se	21.67	41.08	21.5	44	**48.2**	21.5	4.5	0.05
U	32.28	65.73	**66.5**	35	33.4	**66.5**	2.7	2.8
Th	**8.93**	3.53	0	0	0	0	10.7	14.6
Sm	**10.55**	8.22	0	0	0	0	4.5	5.6
Nb	8.96	4.53	**10.63**	0	13	**10.63**	12	1.4
ΣREEs	**145-73**	74-86	95.88	73	139.55	108.125	516.63	400.55
ΣLREEs	**104-61**	49-5	22.5	32.2	67.8	29	141.24	155.65
ΣHREEs	**41.72**	32.91	7.25	0	0	0	12.6	21

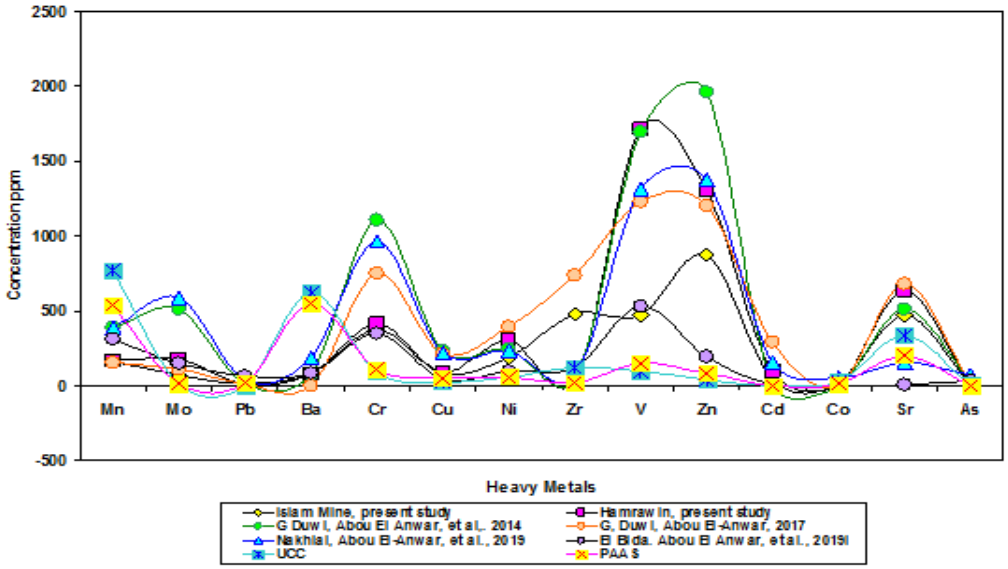

Fig. 13: Distribution the trace elements for the study area and others.

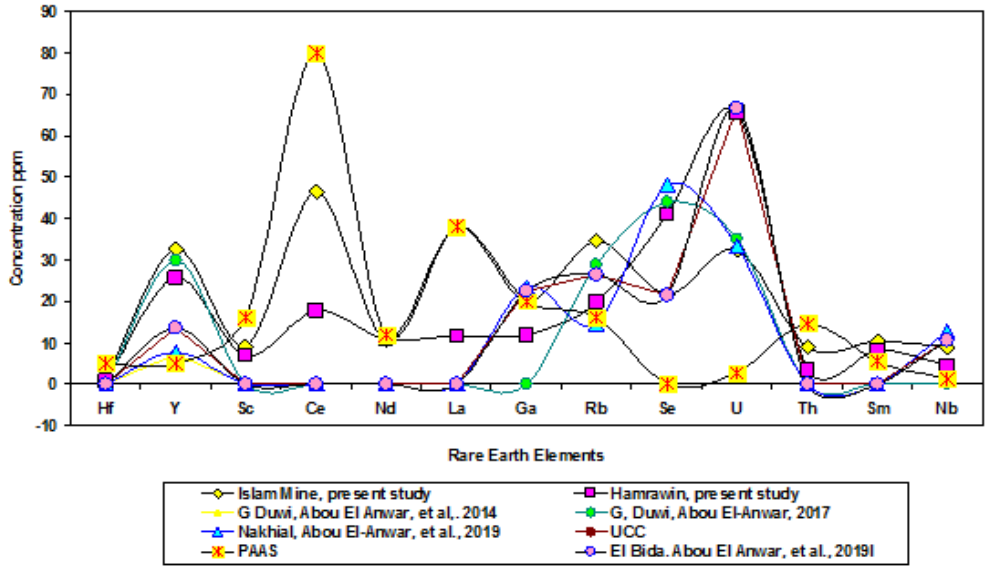

Fig. 14: Distribution the REE elements for the study area and others.

References

[1] Da Silva MF, Fontes MPF, Bellato CR, Neto JOM, Lima HN, Fendorf S. Geochemical signatures and natural background values of rare earth elements in soils of Brazilian Amazon, Environmental Pollution 277 (2021) 116743 Environmental Pollution 277 (2021) 116743

[2] Zuo X, Li C, Zhang J, Ma G, Chen P, Geochemical characteristics and depositional environment of the Shahejie Formation in Binnan oilfield, China. J Geophys Eng 17:539–551(2020)

[3] Ajayi TR, Oyawale AA, Islander, FY, Asubiojo OI, Klein DE, Adediran AI, trace and rare earth elements geochemistry of Oshosun Sediments of Dahomey Basin, Southwestern Nigerian. J. Appl. Sci. 6:2067–2076 (2006).

[4] Nance WB, Taylor SR Rare earth element pattern and crustal evolution in Australian post Archean

sedimentary rocks. GeochimCosmochinActa 40:1539–1557(1974)
[5] Peng B, Andrew R, Zhaoliang S, Changxun Y, Xiaoyan T, Shurong X, Xianglin T, Tan C, Geochemistry of major and trace elements and Pb–Sr isotopes of a weathering profile developed on the Lower Cambrian black shales in central Hunan, China. Applied Geochemistry, 51, 191-203 (2014).
[6] Darwish M., Optimistic hydrocarbon potentialities of the oil shales in Quseir-Safaga land stretch, Egypt. Bull. Fac. Sci. Zagazig Unvi. Zagazig, 5, 409-419 (1984).
[7] Troger D.The oil shales potential of Egypt.Berline Geowissenscafliche Abhandlung (A) 50, 375-380 (1984)
[8] El-KammarAM, Darwish M, Phillip G, El-Kammar MM, Composition and origin of black shales from Quseir area, Red Sea Coast, Egypt. J. Univ. Kuwait (Science), 17, 177-190 (1990)
[9] Ibhrahium DM, Abdel Aziz DA, Awad SA, Abdel Monem AM, Utilization of black shales in earthward recipes. Ceramics International.30, Issuc 6, 829-835 (2004).
[10] Abou El-Anwar EA, El-Sayed MS, Composition of black shale from Quseir, Red Sea, Egypt with emphasis on the sequential extraction of some metals. Bull. NRC, Egypt. 32 (2), 109-131 (2008).
[11] El-Shafeiy M, El-Kammar A, El-Barkooky A, G Philip, A Meyers, Paleo-redox depositional conditions inferred from trace metal accumulation in two Cretaceous-Paleocene organic-rich sequences from Central Egypt, Marine and Petroleum Geology, 73:333-349 (2017).
[12] Baioumy H, Lehmann B, Anomalous enrichment of redox sensitive trace elements in the marine black shales from the Duwi Formation, Egypt: evidence for the late Cretaceous Tethys anoxia. J. Afr. Earth Sci. 133, 7-14 (2017).
[13] Abou El-Anwar EA, Mekky HS, Samy YM, Contribution to the mineralogical, geochemical and provenance of the Cretaceous black shales, Duwi Formation, Quseir–Safaga, Red Sea Coast, Egypt. Egypt J Geol, 58:303–322 (2014)
[14] Abou El-Anwar EA, Mekky HS, Abdel Wahab W, Geochemistry, mineralogy and depositional environment of black shales of the Duwi formation Qusseir area, Red Sea coast, Egypt. Carbonates Evaporites; 34:883-892, https ://doi.org/10.1007/s1314 6-017-0417-7 (2019)
[15] Abou El-Anwar EA, HS Mekky, W Abdel Wahab, Characterization and Depositional Environment of P_2O_5– F- U of Phosphatic Rocks for the Duwi Formation, Qussier- Safaga Region, Red Sea Coast, Egypt. Egyptian Journal of Chemistry, accepted in 16 May 2019 (2019)
[16] Abou El-Anwar EA, Mineralogical, petrographical, geochemical, diageneses and provenance of the Cretaceous Black Shales, Duwi Formation at Quseir-Safaga, Red Sea , Egypt. Egy. J. Petrolum, 26:915-926 (2017).
[17] El-Kammar AM, Zayed M, Amer SA, Rare earths of the Nile Valley phosphorites, Upper Egypt. Chem. Geol., 24, 69-81 (1979).
[18] Abou El-Anwar EA, Lithologic characterization of the phosphorite bearing Duwi Formation (Campanian), South Esna, West Nile Valley, Egypt. Accepted: 25 February 2018, on line March 2018, Carbonates and Evaporites, 34:793–805, https://doi.org/10.1007/s13146-018-0442-1 (2019)
[19] Said R, The Geology of Egypt. A. A. Balkema, Rotterdam, Netherlands p. 734 (1990).
[20] Baioumy HM, Tada R, Origin of Upper Cretaceous phosphorites in Egypt. Cretac.Res. 26, 261-275 (2005).
[21] Chamley H, Clay Sedimentology, Heidelberg, Springer-Verlag, 623 p (1989).
[22] Singer A, The Paleoclimatic interpretation of clay minerals in soils and weathering profiles. Earth – Sci. Rev., 15, 303-326 (1980).
[23] Yuretich R, Melles, M, Starata, B, Grobe H, Clay minerals in the sediments of Lake Baikal: a useful climate proxy. J Sediment Res 69(3), 588-896 (1999)
[24] Abou El-Anwar EA, Mineralogical, petrographical, geochemical, diageneses and provenance of the Cretaceous Black Shales, Duwi Formation at Quseir-Safaga, Red Sea, Egypt. (Carbonates Evaporites http://dx.doi.org/10.1016/j.ejpe.2016.06.005) (2017)
[25] Taylor SR, McLennan SM, The Continental Crust: Its Composition and Evolution. Blackwell, Oxford, 46-92 (1985).
[26] Rudnick RL, Gao S, Composition of the Continental Crust. Treatise On Geochemistry, 3, 1-64 (2014).
[27] Blumenberga M, Thiela V, Riegela W, Linda K, R. Joachim, Biomarkers of black shales formed by microbial mats, Late Mesoproterozoic (1.1 Ga) Taoudeni Basin, Mauritania, Precambrian Research, 196-197: 113-127 (2012).
[28] Abou El-Anwar EA, Petrography, geochemistry and genesis of the Upper Eocene carbonate terraces

(II and III), Qasr El-Sagha Formation El-Fayeum, Egypt. Sedimentology of Egypt, 13, 243-260 (2005).
[29] Abou El-Anwar, E.A., 2006, Petrography, geochemistry and genesis of some Middle Eocene rocks at Qattamia area, Cairo-Suez Road, Egypt. NRC, Egypt. 31 (6), 519-543.
[30] Abou El-Anwar EA, Petrographical, geochemical and diagenetic studies of the Middle Eocene carbonates, Mokattam Formation of Darb El-Fayium area. Int. Conf. on Geological and Engineering, Paris, France, 24-26 August, 80, 1315-1325 (2011)
[31] Abou El- Anwar EA, EL-Wekeil SS, GaafarFSh, Contribution to the mineralogy, geochemistry, and provenance of the Lower Eocene Esna shale in the Farafra Oasis, Western Desert, Egypt, J. of Applied Sciences Research. 9(8), 5344-5369, (2013).
[32] Angerera T, Kerrichb R, Steffen G, Geochemistry of a komatiitic, boninitic, and tholeiitic basalt association in the MesoarcheanKoolyanobbing greenstone belt, Southern Cross Domain, Yilgarncraton: Implications for mantle sources and geodynamic setting of banded iron formation, Precambrian Research, 224: 110-128 (2013).
[33] Xiugen Fu, Wang Y, Zeng F, Tan E, Feng X. REE geochemistry of marine oil shale from the Changshe Mountain area, northern Tibet, China. Int J Coal Geol 81,191-199 (2010)
[34] Marz C, Inorganic geochemical redox proxies-indicators for rapid palaeoenvironmental changes and related diagenetic processes in recent and ancient marine sediments (Ph D thesis), University of Bremen (2007)
[35] Ross DJK, Bustin RM. Investigating the use of sedimentary geochemical proxies for palaeoenvironment interpretation of thermally mature organic-rich strata: examples from the Devonian-Mississippian shales, Western Canadian Sedimentary Basin. ChemGeol 260, 17-19 (2009)
[36] Swanson V, A Review Geology and Geochemistry of Uranium in Marine Black Shales, United States Government Printing Office, Washington, 112p (1961)
[37] Armands G, Geochemical studies of uranium, molybdenum and vanadium in a Swedish alum Shale. Stockholm Contrib. Geol.27, 148 (1972).
[38] Venter R, Boylett M, The evaluation of various oxidants used in acid leaching of uranium. Hydrometallurgy Conference, The Southern African Institute of Mining and Metallurgy, 445-456 (2009).
[39] Waite TD, Davis JA, Payne TE, Waychunas GA. Uranium (VI) adsorption to ferrihydrite: application of a surface complexation model. GeochimCosmochimActa, 58, 5465-5478 (1994).
[40] Bots P, Behrends T. Uranium mobility in subsurface aqueous systems: the influence of redox conditions. Mineralogical Magazine, 72, 381-384 (2008).
[41] Bata T. Evidences of widespread cretaceous deep weathering and its consequences: a review. Earth Sci Res. 5(2), 69 (2016)
[42] Song HJ, Wignall PB, Tong JN, Bond DPG, Song HY, Lai XL, Zhang, K Wang, HM, Chen YL, Geochemical evidence from bio-apatite for multiple oceanic anoxic events during Permian–Triassic transition and the link with end-Permian extinction and recovery. Earth Planet. Sci. Lett. 323-324, 12-21 (2012).
[43] Wignall PB, Twitchett RJ. Oceanic Anoxia and the End Permian Mass Extinction.Science 272, 1155-1158 (1996).
[44] Abou El-Anwar EA, Salman AS, Mousam DA, Aita SK. Geochemical and Mineralogical Evaluation of Black Shale and its Hydrocarbon Potentiality, Southwest Sinai, Egypt, Egypt. J. Chem. 63 (12) 5055 - 5070, DOI: 10.21608/EJCHEM.2020.44732.2907 (2020)
[45] Abou El-Anwar EA, Abdelhafiz MA, Salman AS. Rare earth and trace elements enrichment and implications in black shales of Safaga-Qussier sector, Egypt, Journal of African Earth Sciences 188 - 104482 (2022)
[46] Abou El-Anwar EA, Abd El Rahim SH. Mineralogy, geochemistry and origin of the phosphorites at Um El-Huwtat mine, Quseir, Central Eastern Desert, Egypt, Carbonates and Evaporites, (2022) 37:16 (2022).
https://doi.org/10.1007/s13146-022-00759-4
[47] Abou El-Anwar EA, Salman AS, Mousa DA, Aita SK, Makled W, Gentzis T Organic Petrographic and Geochemical Evaluation of the Black Shale of the Duwi Formation, El Sebaiya, Nile Valley, Egypt. Minerals, Accepted: 8 December 2021 Published: 14 December (2021).
[48] Turekian KK. Nickel. In: Wedepohl, K.H. (Ed.), Handbook of Geochemistry, II/3. Springer, Berlin, 28-K-1–28-L-3 (1978)
[49] Dhannoun HY, Al- Dlemi AMS, The relation between Li, V, P2O5, and Al2O3 contents in marls and mudstones as indicators of environment of

deposition. Arabian Journal of Geosciences 6, 817-823 (2013).
[50] Adegoke AK, Abdullah WH, Hakimi MH, Yandoka BMS, Mustapha KA, Aturamu AO, Trace elements geochemistry of kerogen in Upper Cretaceous sediments, Chad (Bornu) Basin, northeastern Nigeria: origin and paleoredox conditions. J. Afr. Earth Sci. 100, 675-683 (2014).
[51] Wright J, Schrader H, Holster W, Paleoredox variations in ancient oceans recorded by rare earth elements in fossil apatite. GeochimicaetCosmochimicaActa 51, 631-644 (1987).
[52] Jones B, Manning DAC, Composition of geochemical indices used for the interpretation of paleoredox conditions in ancient mudstones. Chem. Geol. 111, 111-129 (1994).
[53] Galarraga F, Reategui K, Martïnez A, Martínez M, Llamas JF, Márquez G, V/Ni ratio as a parameter in palaeoenvironmental characterisation of non-mature medium-crude oils from several Latin American basins. Journal of Petrological Science and Engeneering, 61, 9-14 (2008).
[54] Pi DH, Jiang SY, Luo L, Yang JH, HF Hong-Fei Ling, Depositional environments for stratiform with erite deposits in the Lower Cambrian black shale sequence of the Yangtze Platform, southern Qinling region, SW China: Evidence from redox-sensitive trace element geochemistry. Palaeogeography, Palaeoclimatology, Palaeoecology, 398, 125-131 (2014).
[55] Jeon J, Shin D, Im H, Depositional environment of redoxsensitive trace elements in the Metalliferous Black Slates of the Okcheon Metamorphic Belt, South Korea. Geosci J 24(2), 177-193 (2020)
[56] Jiang SY, Chen YQ, Ling HF, Yang JH, Feng HZ, Ni P, Trace and Rare Earth Element Geochemistry and Pb-Pb Dating of Black Shales and Intercalated Ni-Mo-PGE-Au Sulfide Ores in Lower Cambrian Strata, Yangte Platform, South China. Mineralium Deposita 41, 5, 453-467 (2006).
[57] Xin H, Jiang S, Yang J, Wu H, Pi D, Rare earth element geochemistry of phosphatic rocks in Neoproterozoic Ediacaran Doushantuo Formation in Hushan section from the Yangtze Gorges area, South China. J. of Earth Sciences.27, 204-210 (2016).
[58] Boote DRD, Clark-Lowes DD, Traut MW, Palaeozoic petroleum systems of North Africa. In: Macgregor, D.S., Moody, R.T.J., Clark-Lowes, D.D. (Eds.), Petroleum Geology of North Africa, vol. 132. Geological Society of London Special Publications, 7-68 (1998).
[59] Lee YI. Geochemistry of shales of the Upper Cretaceous Hayang Group, SE Korea: Implications for provenance and source weathering at an active continental margin. Sedimentary Geology, 215, 1-12 (2009).
[60] Piper DZ, Seawater as the source of minor elements in black shales, phosphorites and other sedimentary rocks, Chemical Geology, 114,95-114 (1994).
[61] McLennan SM, Nance WB, Taylor SR, Rare earth element-thorium correlations in sedimentary rocks, and the composition of the continental crust. Geochem. Cosmochim. Acta 44, 1833-1839. https://doi.org/10.1016/0016-7037(80)90232-X (1980).
[62] Jiang YB, Ji HB. Rare earth geochemistry in the dissolved, suspended and sedimentary loads in Karstic Rivers, Southwest China. Environ. Earth Sci., 66(8): 2217 (2012).
[63] Yusoff ZM, Ngwenya BT, Parsons I, Mobility and fractionation of REEs during deep weathering of geochemically contrasting granites in a tropical setting, Malaysia. Chem. Geol. 349, 71 (2013)
[64] Gao P, Zheng YF, Zhao ZF, Distinction between S-type and peraluminousItype granites: zircon versus whole-rock geochemistry. Lithos.258-259, 77-91 (2016).
[65] Nesbitt HW, Young GM, Early Proterozoic climates and plate motions inferred from major element chemistry of lutites, Nature, 299, 715-717 (1982).
[66] Fedo CM, Nesbit HW, Young GM, Unravelling the effect of potassium metasomatism in sedimentary rocks and paleosols, with implications of paleoweathering conditions and provenance, Geology 23, 921–924 (1995).
[67] Fedo CM, Eriksson K, Krogstad EJ, Geochemistry of shale from the Archean (~ 3.0 Ga) Buhwa Greenstone belt, Zimbabwe: Implications for provenance and source area weathering: Geochimicaet Cosmochimica Acta, 60(10), 1751-1763 (1996)
[68] McLennan SM, Hemming S, McDaniel DK, Hanson GN, Geochemical Approaches to Sedimentation Provenance and Tectonics. In: Processes Controling Composition of Clastic Sediments –Johanson, M.J. and A. Basu(Eds.) Geological Society of American, Special Paper, USA.,. 21-40 (1993)

[69] Cox R, Lower DR, Cullers RL, The influence of sediment recycling and basement composition on evolution of mudrock chemistry in the southwestern United States. Geochim. Cosmochim. Acta, 59, 2919-2940 (1995).

[70] Barshad I, The effect of variation in precipitation on the nature of clay mineral formation in soils from acid and basic igneous rocks. Proc. Int. Clay, 167-173 (1966)

[71] Shi C, Cao J, Bao J, Zhu C, Jiang X, Wu M, Source characterization of highly mature pyrobitumens using trace and rare earth element geochemistry: sinian-Paleozoicpaleo-oil reservoirs in South China. Org. Geochem. 83-84, 77-93 (2015).

[72] Wang Min-fang, Jiao Yang-quan, Wang Zheng-hai, Yang Qin, Yang, and Sheng-ke, Recovery paleosalinity in sedimentary environment – an example of mudsone in Shuixigou group, southwestern margin of Turpan-Hami basin. Xin Jiang Petroleum Geology 12 (6), 719-722 (2005)

[73] Floyd PA, Leveridge BE, Tectonic environment of the Devonian Gramscatho basin, south Cornwall: framework mode and geochemical evidence from turbiditic sandstones. J. Geol. Soc. 144, 531-542 (1987).

[74] Feng R, Kerrich R, Geochemistry of fine-grained clastic sediments in the Archean Abitibi greenstone belt, Canada: implications for provenance and tectonic setting. Geochemicaet Cosmochemica Acta 54, 1061-1081 (1990).

[75] Roser BP, Korsch R., Determination of tectonic setting of sandstone-mudstone suites using SiO2 content and K2O/Na2O ratio. J. Geol. 94, 635-650 (1986).

[76] Bhatia MR, Plate tectonics and geochemical composition of sandstones. J. Geol. 91, 611-627 (1983).

[77] Jacobson AD, Blum JD, Chamberlain CP, Craw D, Koons PO, Climatic and tectonic controls on chemical weathering in the New Zealand Southern Alps. Geochim. Cosmochim. Acta, 37, 29-46 (2003).

[78] Boggs Jr S, Boggs S, Petrology of Sedimentary Rocks. Cambridge university press, New York, p. 600 (2009)

[79] Roy DK, Roser BP, Climatic control on the composition of Carboniferous- Permian Gondwana sediments, Khalaspir basin, Bangladesh. Gondwana Res. 23, 1163-1171 (2013).

[80] Ben-Awuah J, Padmanabhan E, Sokkalingam R, Geochemistry of Miocene sedimentary rocks from offshore West Baram Delta, Sarawak Basin, Malaysia, South China Sea: implications for weathering, provenance, tectonic setting, paleoclimate and paleoenvironment of deposition. Geosci.J. https://doi.org/10.1007/s12303- 016-0056-3 (2017).

[81] Wanas HA, Abdel-Maguid NM, Petrography and geochemistry of the Cambro-Ordovician Wajid Sandstone, southwest Saudi Arabia: implications for provenance and tectonic setting. Journal of Asian Earth Sciences 27, 416-429 (2006).

[82] Abou El-Anwar EA, Mineralogical and Geochemical studies on Soils and Nile Bottom Sediments of Luxor-Aswan Area, South Egypt, Bulletin of the National Research Centre, Accepted Date:19 April 2021 (2021)